Available online at www.sciencedirect.com

ScienceDirect

Journal of Ocean Engineering and Science 2 (2017) 161–171

www.elsevier.com/locate/joes

The response of a semisubmersible model under focused wave groups: Experimental investigation

Michael Banks, Nagi Abdussamie*

National Centre for Maritime Engineering and Hydrodynamics, Australian Maritime College, University of Tasmania, Launceston, TAS 7250, Australia

Received 2 May 2017; accepted 28 July 2017
Available online 3 August 2017

Abstract

In recent years, extreme wave events have occurred more frequently than have been predicted using theoretical methods. It is, therefore, a requirement to investigate the impact of these events on coastal and offshore structures. This paper reports on results of an experimental investigation into the interaction between unidirectional waves and a horizontally moored semisubmersible model. The target crest height was created at a focal point and time using the focused wave technique. Different values of wave steepness were tested in order to ascertain the nonlinear effects on the quality of waves generated by a piston-type wavemaker. The measured crest height was in good agreement with the theoretical one within 4% relative error. The magnitudes of heave and pitch motions of the model were found to increase as the wave steepness increased. Overall, the paper contributes towards establishing the application of focused wave technique to floating offshore platforms.

Keywords: Focused wave; Offshore platforms; Dynamic response.

1. Introduction

The design of offshore structures against extreme sea states such as hurricanes/cyclones is one of the greatest challenges in marine and offshore industry. Loads generated by such events can be immense and difficult to predict with the potential to cause platform destruction and fatalities. The necessity of design for these events with a high degree of accuracy is critical for both economic and safety aspects. An example of such events occurred on the 1st of January 1995; an extreme wave event was recorded at the Draupner platform located in the North Sea. The recorded wave had a maximum crest height of 18.6 m (η_{max}) which largely exceeded the 100-year significant wave height of 12 m in the North Sea [1]. This record is considered to be one of the most reliable data of a rogue/freak wave as examined by the resultant damage to the deck of the platform [2,3].

The risks posed by rogue waves have recently been highlighted by a series of vessels related incidents with some resulting in fatalities [3,4]. Hurricane and typhoon actions, in areas such as the Gulf of Mexico and the Australian North West Shelf, create a situation where a continued evolution of testing methods is required.

The crest–trough height H of an extreme or rogue wave can be defined as twice the significant wave H_s or the wave crest height (η_{max}) is 1.25 times H_s [5]. Exactly how extreme waves occur is subject to debate; given their finite nature and varying characteristics, accurate analysis is difficult. Some of the possible mechanisms causing extreme waves are; wave–wind interaction, wave–bottom interaction (spatial focusing), wave–current interaction and wave–wave interaction. Each of these possibilities can be used to explain the extreme steepness of the wave and higher than average wave energy present in an extreme wave. The work was undertaken by Cui et al. [6] on spatial focusing noting the impact that refraction, reflection and shoaling have on characteristics of a focused wave. It was found that the greatest effect was on high and low-frequency wave components, concentrating them and affecting the

* Corresponding author.
E-mail address: nagia@utas.edu.au (N. Abdussamie).

http://dx.doi.org/10.1016/j.joes.2017.07.003

focus wave characteristics. Touboul et al. [7] found through numerical and experimental testing that there is a significant increase in the transfer of energy and momentum from the wind to waves in extreme wave events effectively enhancing the extreme waves.

Several methods have been developed for creating realistic sea-states for model testing. Baldock et al. [8] used superposition of a series of small first order waves to create a focused wave at a design point, described as wave convergence. It was found that the waves tended to fully develop further away from the wave maker paddle due to nonlinear wave effects. Chaplin [9] and later Schmittner et al. [10] used a phase and amplitude iteration process to create extreme wave events in testing. The methodology used was based on first order linear wave theory; using the assumption that energy propagation is relative to the instantaneous frequency of the wave leaving the wave maker paddle and using frequency modulation to create a focused wave. It was found that only one or two iteration steps were required to produce what was considered realistic reproductions of a recorded wave train once the methodology was established. An interesting side note is that Schmittner et al. [10] found that the proposed iteration method requires little knowledge of wave maker transform functions treating the wave maker as effectively a "black box" and that only input and output signals are being considered. Fernández et al. [11] created focused waves with a self-correcting designed to account for both varying water depths and wave non-linearity. The premise of the self-correcting method is to eliminate extra potential frequencies created when constructing the wave profile back to the wave maker from the focused wave. Crossing seas or bi-directional sea states have also been explored; Cook [12] used the method to assess loadings on a fixed Tension Leg Platform (TLP). The location and timing of focused wave required a large number of iterations.

The NewWave theory, i.e., focused wave technique was first developed by Tromans et al. [13]. Taking a known wave spectrum, a deterministic first order focused wave can be created. The methodology is to superimpose a series of smaller first order waves focusing them to a design wave at the desired point. Cassidy [14] took this further creating a constrained NewWave to account for the randomness of a sea state whilst still maintaining the chosen design wave. A further development has been to add phase iteration to the NewWave theory. Gao et al. [15] used this method, progressively creating a more accurate representation via iteratively altering the initial phase angle. The main advantage of the NewWave theory is that it creates a focused/design wave in a very short period of time. When using this method Ning et al. [16] only required a 20 s sample time for a simply focused wave whilst Deng et al. [17] used only a 30 s sample to create a scale sea state of the New Year wave. This technique can provide an attractive option when coupled with the cost of facility hire. Similarly, the NewWave theory can be used in a numerical setting as done by Gao et al. [18], Lu et al. [19] and Westphalen et al. [20].

The predominate use of focused waves has been with fixed structures; Westphalen [21] used a design focused wave to assess the loads on fixed offshore wave energy devices. Cassidy et al. [22] applied a constrained NewWave sea state to jack-up units. Gao et al. [18] and Deng et al. [17] applied deterministic freak waves to applying the loads on horizontally fixed cylinders. Some analysis has been undertaken on using floating structures; Ransley [5] applied the NewWave theory to assess extreme loads on a moored buoy and a floating wave energy device. Hu and Causon [23] used the Cartesian cut cell method to analyse both a fixed horizontal cylinder in a numerical wave tank and floating bobber. The focus bias appears to be both evident in experimental and numerical testing with fixed structures receiving the majority of work when applying the focused wave theory.

The scope of this paper is to implement the focused wave technique to model test facilities with a piston-type wave maker and to investigate the interaction between a floating body and generated focused wave group events. A short-time wave record was taken from Ning et al. [16], as it provided a practical starting point towards more realistic wave events such as the New Year wave. Firstly, wave calibration was conducted without the model being in the tank to ascertain the uncertainty involved in wave generation. Secondly, a series of wave impact tests were performed. Uncertainty analyses of wave elevations and model's motions were presented, and the experimental results were discussed.

2. Focused wave technique

The focused wave theory is a method of using phase shift to place a design wave elevation at a chosen point and time (creating a focused wave). This works through decomposing a finite number of first order components of a sea spectrum using fast Fourier transform (FFT) and adding a design focal time (t_f) and design focal distance (x_f) [21]. The focused wave elevation formula can be written as:

$$\eta(x,t) = \sum_{n=1}^{n=N} a_n \cos\left(k_n\left(x - x_f\right) - \omega_n\left(t - t_f\right) + \varepsilon_n\right) \tag{1}$$

In which a_n is the wave amplitude, k_n is the component wave number obtained using the linear dispersion relation, and ε_n is the initial component phase. In this paper, the total focusing crest height $\eta_{\max}$ is defined as the input parameter $\eta_{\max} = \sum_{n=1}^{n=N} a_n$. It should be noted that when $x_f = t_f = 0$, the resulted signal will be identical to the original one.

In order to generate a focused wave in a physical wave tank, the position of paddle of wavemaker x can be taken as 0. In addition, to implement the focused wave technique Eq. (1) must be modified to create a time history of wavemaker paddle displacement. In this work, 16-paddle piton-type wavemaker was used to generate unidirectional focused waves (see Fig. 1). The time history of a paddle stroke is given by [24]:

$$S(t) = \sum_{n=1}^{n=N} \frac{a_n}{Tr} \sin\left(k_n x_f - \omega_n\left(t - t_f\right) - \varepsilon_n\right) \tag{2}$$

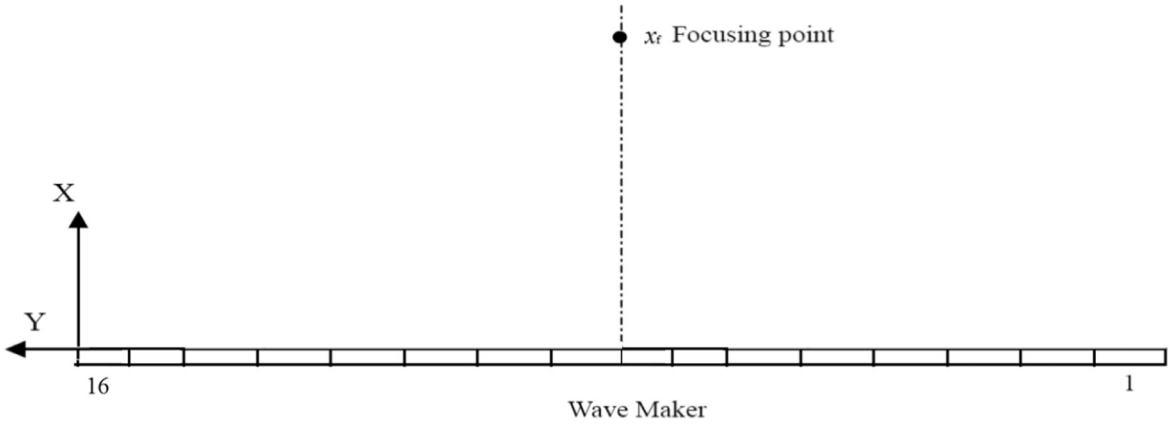

Fig. 1. Definition sketch showing 16-paddle wavemaker and the location of the focused point.

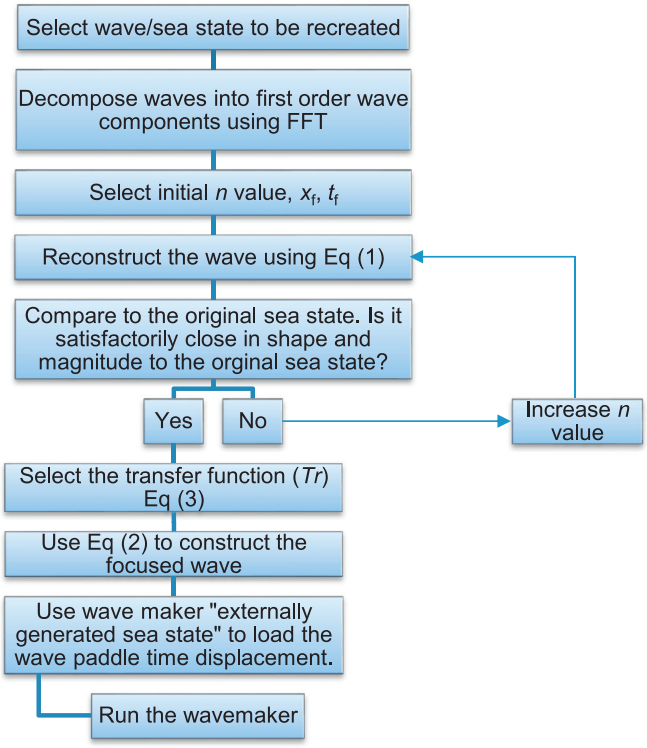

Fig. 2. Testing procedure flowchart for creating focused wave groups in a physical wave tank.

The transfer function (Tr), i.e., the relationship between the wave height and the stroke of the wavemaker for a piston-type wavemaker is given by for each component [25]:

$$Tr = \frac{H}{S} = \frac{2(\cosh 2kh - 1)}{\sinh 2kh + 2kh} \tag{3}$$

where h is water depth. As noted by Gao et al. [15], there is a significant difference in the effectiveness of wavemakers in shallow, intermediate and deep water conditions. Fig. 2 shows the testing procedure followed in this work to generate a focused wave.

It should be noted that flap type wavemakers are better suited to only deep-water conditions whilst piston types are effective in shallow and intermediate water depths. Taking note from data collected by Ursell et al. [26] the curve produced by theoretical wavemaker displacements is not always smoothed and thus may produce exact linear transforms of stroke to wave amplitude.

3. Tank experiments

A series of model tests were conducted in the Model Test Basin (MTB) of the Australian Maritime College (AMC). The tank is 35 m long, 12 m wide and can be operated at different water depths of up to 1.0 m. The tank is equipped with wavemaker of 16 electrically driven piston-type paddles. An artificial beach is located at the opposite end of the tank in order to minimise wave reflections. The beach dimensions are 2975 mm long and 470 mm high at the far end. The tank experiments reported in this paper were executed using the following procedure:

1- *Wave calibration tests*—in which the focused wave technique was implemented; different wave probes were used and the evolution of wave elevation along the tank was investigated.
2- *Wave impact tests*—in which a generic semisubmersible model was setup and subjected to the wave events generated in step 1; rigid-body motions of the model were then measured.

3.1. Wave calibration tests

In order to experimentally measure a focused wave and to establish a testing procedure, a short-time wave record taken from Ning et al. [16] was used. The design wave crest (η_{max}) is a reproduction of case two used by Ning et al. [16]. Testing the air gap of the model was undertaken by increasing the amplitude of focused waves, η_{max}. For the focused wave $n = 16$ evenly staggered between 0.6 and 1.3 Hz. The focus was on achieving a repeatable trend and maximum wave crest height

Table 1
Test matrix.

Condition	Target η_{max} (mm)	Frequency range (Hz)
1	63.2	0.6–1.3
2	69.5	0.6–1.3
3	75.8	0.6–1.3
4	82.2	0.6–1.3
5	88.5	0.6–1.3

Table 2
Distance of wave probes along the tank measured from the paddle.

Wave probe (WP)	Location (x) mm
1	3000
2	10,000
3	11,000
4	12,000

Table 3
Model's main particulars.

Parameter	Model dimension
Column diameter	200 mm
Pontoon size: length × height × width	408 × 92 × 92 mm
Column spacing	608 mm
Column height	505 mm
Deck size: length × width × height	608 × 608 × 210 mm
Draft	305 mm
Deck clearance	120 mm
Mass displacement	52.20 kg
Vertical centre of mass	5.00 mm above SWL
Mass moment of inertia (I_{xx}, I_{yy}, I_{zz})	(5.23, 5.23, 5.63) kg m^2

in every run. To assess the impact of the focused wave on the motions of the model the original signal was increase progressively by 10% as presented in Table 1. The run period remained the same throughout testing as did the frequency band.

Once the frequency and spectral density of each wave component was obtained using FFT, the time history file of the paddle displacement was created. The selected wave elevation has a maximum crest height of 63.2 mm, peak frequency of 0.83 Hz. The design focal point (x_f) was taken as 3000 mm (1.5λ_p). The focal time (t_f) was taken as $8T_p$ where T_p (T_p = 1.2 s) is the wave spectrum peak period. The total run time of each focused wave group was 20 s with a sampling frequency of 20 Hz.

Four capacitance-type wave probes were used to capture the wave elevation and its evolution along the tank. Table 2 presents the location of wave probes relative to the initial position of the paddle where each wave probe was placed at approximately 600 mm from the tank sidewall (Fig. 3).

3.2. Wave impact tests

A generic model of a semisubmersible platform was designed and constructed in order to investigate wave–structure interaction due to user-defined wave packets. As shown in Fig. 4, the model consists of two main modules namely hull module (4 columns and 4 pontoons) and topside deck module (box-shaped deck), see Table 3. The model's centroid was setup at the longitudinal centreline of the tank approximately 11,000 mm away from the paddle, i.e., in-line with WP#3.

A motion tracking system (Qualisys) was used to capture the model's motions namely heave, pitch and surge. In order to maintain the position of the model throughout model tests, an arrangement of horizontal soft mooring system was used for this purpose. A mooring line of approximately 8250 mm long was attached on each side of the model at its pontoon centreline. The anchor point was a 3-pully arrangement attached to the tank side. A light mass of approximately 0.51 kg was then connected to the end of the mooring line (Fig. 5). Such arrangement was found to minimise the horizontal drift of the model but allowing it to move freely in at least three degrees of freedom.

Table 4
Natural periods and damping ratios of the model.

Motion	Measured (s)	Predicted (s)	Error (%)
Heave	1.61	1.73	7.45
Pitch	4.02	4.10	2.00

Table 5
Results of uncertainty analyses for η_{max} during wave calibration (values were averaged over 13 repeated runs).

Statistical value	WP#1	WP#2	WP#3	WP#4
Mean (mm)	61.35	57.58	58.54	58.52
Standard deviation (mm)	0.35	0.32	0.45	0.44
Error (%)	2.92	8.89	7.37	7.40

Table 6
Standard deviations of maximum magnitudes of pitch and heave motions (results obtained using 5 repeated runs).

Condition	Pitch standard deviation (°)	Heave standard deviation (mm)
1	0.12	0.44
2	0.09	0.51
3	0.17	0.10
4	0.18	0.14
5	0.05	0.38

3.3. Free decay tests

Free decay tests in heave and pitch degrees of freedom were conducted to determine the natural periods. The time traces were analysed using the logarithmic decrement method. Table 4 presents the experimental results of the free decay tests along with the predicted natural periods. A relative error of approximately 7.5% and 2% between the predicted and measured results was obtained for the heave and pitch natural periods, respectively. Such a discrepancy can be attributed the simplification in the added mass estimation.

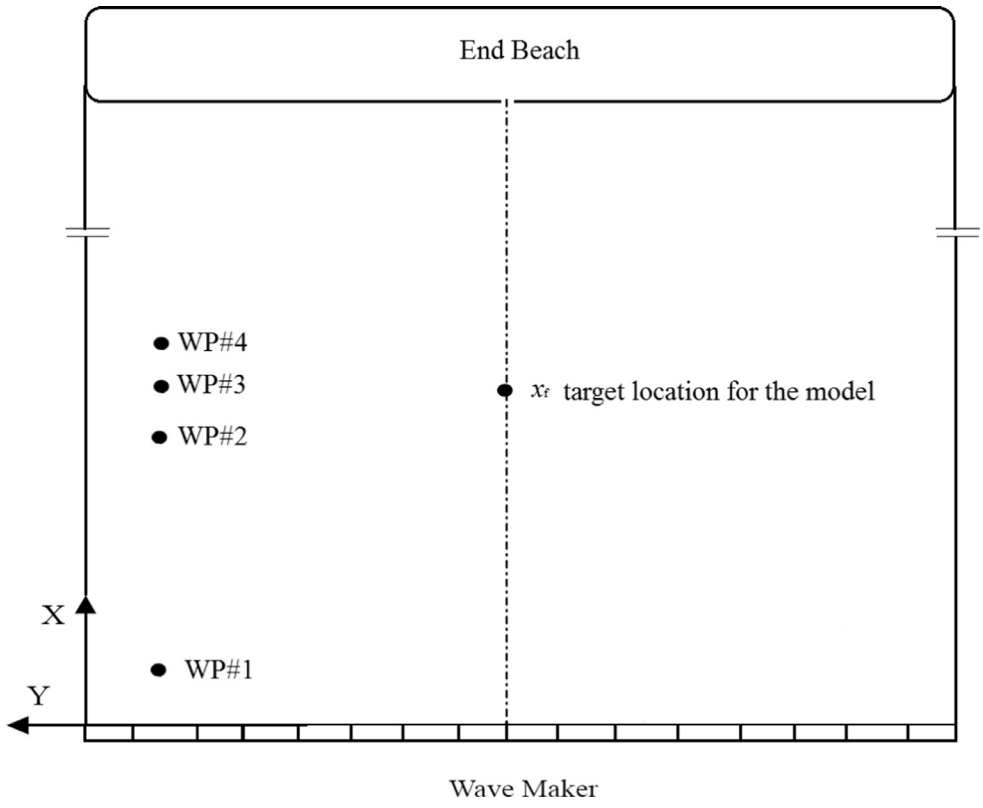

Fig. 3. Top view showing the location of wave probes used during wave calibration (not to scale).

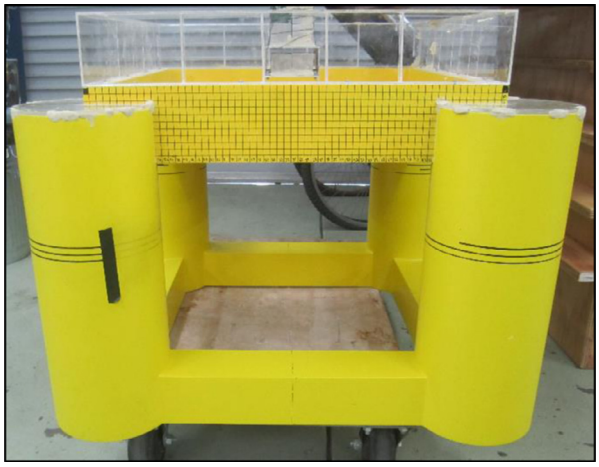

Fig. 4. Photograph showing the semisubmersible model prior to model tests.

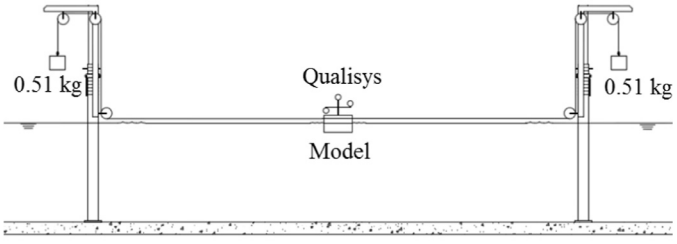

Fig. 5. Profile view (*yz* plane) showing the semisubmersible model attached to a soft mooring system.

4. Data analyses

4.1. Wave elevations

Table 5 presents the mean wave amplitude and standard deviation for the 13 calibration runs for condition 1 (target $\eta_{max} = 63.2$ mm). The relative error between the mean incident probe amplitude and the design amplitude was approximately 3%. The relative error increased to 9% at WP#2. The rise in the mean amplitude between wave probes WP#2–WP#4 suggests a focal point near to WP#3. This is in agreement with the focal point used by Ning et al. [16] at 11.4 m.

A decrease in amplitudes can be noted as the wave propagated down the basin relative to the design and incident wave amplitude. From Fig. 6 it can be seen the trend of surface elevation at each wave probe proved to be constant with little variation.

It can be noted that the increase in variation in wave peaks between differing probes with WP#3 exhibiting the greatest standard deviation. This might be caused by the wave dissipation effects and intermediate water depths; while noted these effects are not considered due to testing restrictions. The generalised trend of produced wave is not an exact reproduction of the original focused wave. Though the trend is similar the extreme troughs are significantly reduced; this again is a likely effect of intermediary water depths. The design focus wave peak itself is far closer between the design and incident probe recorded signal with an average peak error of only 2.92%.

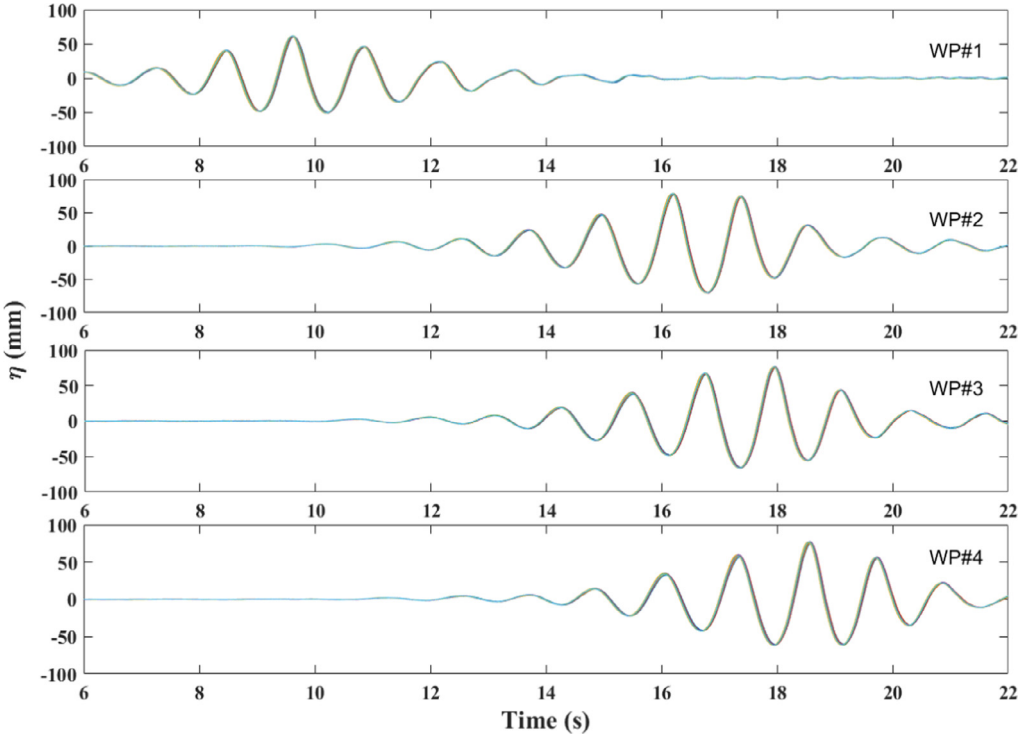

Fig. 6. Time history of measured wave elevations along the tank for wave calibration using 13 repeated runs (Target η_{max} = 63.2 mm).

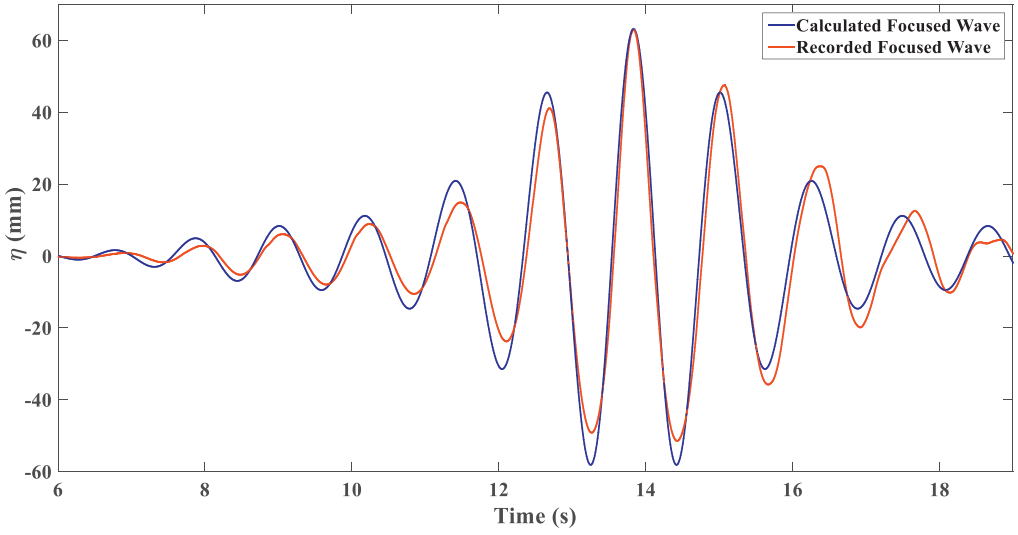

Fig. 7. Time history of wave elevations measured at the incident wave probe (WP#1).

The presented errors are possibly a function of water depth, wave dissipation or due to wavemaker systematic inaccuracy in the calculated transfer function. Similar errors have been experienced in focused wave creation in other test facilities and require further iterations to fully explore [10,16,24]. Another possibility is that the actual displacement of the wavemaker paddle does not adhere to the theoretical curve as seen by Ursell et al. [26] (Fig. 7).

4.2. Motions

Qualitatively the motions (heave and pitch) of the model were found to be consistent throughout testing. Figs. 8 and 9 show the heave and pitch of the model using 5 repeated runs, respectively. The heave motion magnitudes of the model were almost constant throughout all conditions with a maximum peak standard deviation of 0.51 mm (Table 6).

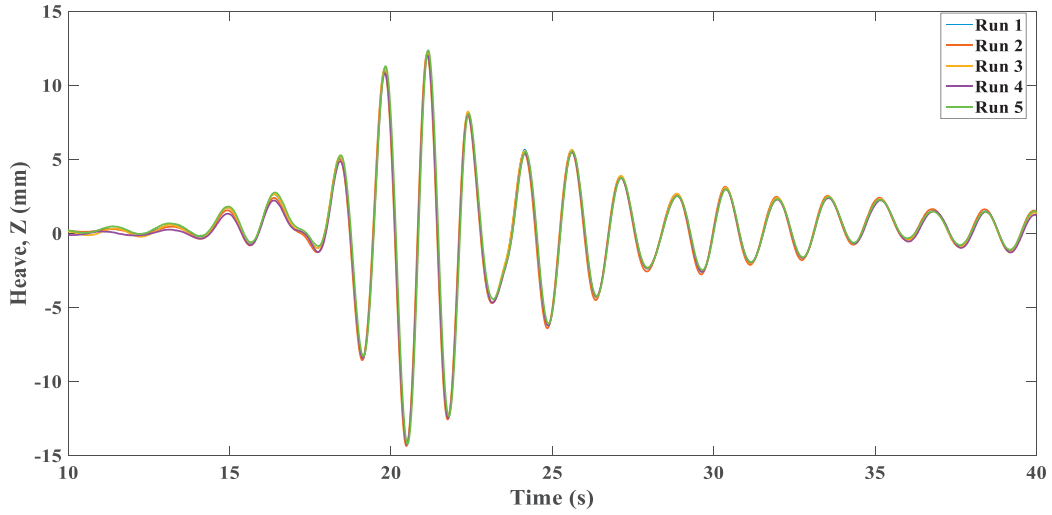

Fig. 8. Time history of measured heave motions using five repeated runs for condition 1 (Target η_{max} = 63.2 mm).

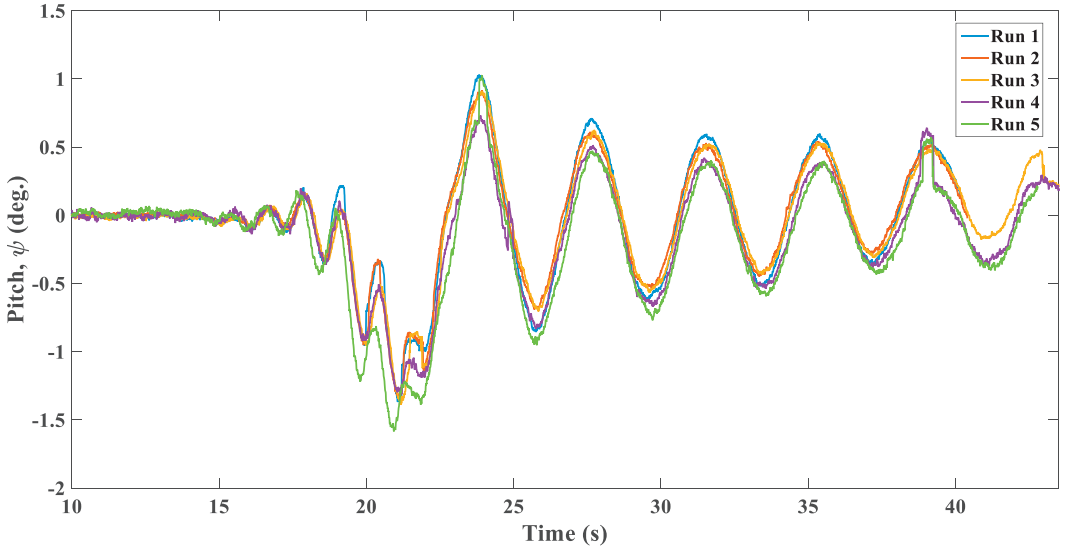

Fig. 9. Time history of measured pitch motions using five repeated runs for condition 1 (Target η_{max} = 63.2 mm).

Whilst the pitch motion of the model was found to vary in extreme values to a more significant degree, although the general pattern of the motion is consistent throughout (Fig. 9). As can be seen from Table 6 the actual variation for the pitching data remains low throughout all of the recorded runs. It is worth noting that the recorded peak values of pitch motion were relatively small which may have some effect on the accuracy of Qualisys system. However, it is expected that the design focus waves will provide relatively consistent results in an experimental setting as experienced by Deng et al. [24] and Ning et al. [16].

5. Results and discussion

The time history of wave elevation (η) at WP#3, heave motion (Z) and pitch motion (ψ) for conditions 1, 3 and 5 are discussed below. For all conditions tested, the maxima and minima values of Z and ψ along with the measured and target crest height η_{max} are presented in Table 7.

By referring to Figs. 10 and 11, it is notable that the wave elevation did not conform to the designed focus wave; the peak wave effectively shifted in the wave set, moving to the next crest and diminishing in amplitude. The relationship between all three large peaks changed with significantly more energy seeming to have moved to the back of the wave set. This would likely be due to the effects of non-linear wave interaction as the waves are propagating down the basin. However, for condition 5 the extreme peak (η_{max}) did not shift in the wave packet, more closely modelling the design wave (still appearing to underestimate the target η_{max} (−4.0%) as have all conditions). The method of increasing the wave sets was to increase the calculated wavemaker paddle displacement time series by progressive 10% intervals. Doing this precluded a change in the calculated wave length. As the transfer function (Eq. (3)) is calculated relative to the depth of the test basin

Table 7
A summary of wave crest height and model's motions results for all conditions.

Condition	η_{max} at WP#3 (mm)			Heave motion (mm)		Pitch motion (°)	
	Measured	Target	Error (%)	Max	Min	Max	Min
1	60.10	63.20	−4.00	11.34	−13.98	0.80	−1.61
2	68.72	69.52	−1.20	13.16	−15.97	1.08	−1.87
3	75.02	75.84	−1.10	14.27	−17.64	1.27	−1.89
4	81.45	82.16	−0.90	15.35	−20.32	1.17	−2.24
5	87.20	88.48	−1.50	16.42	−22.65	1.39	−2.68

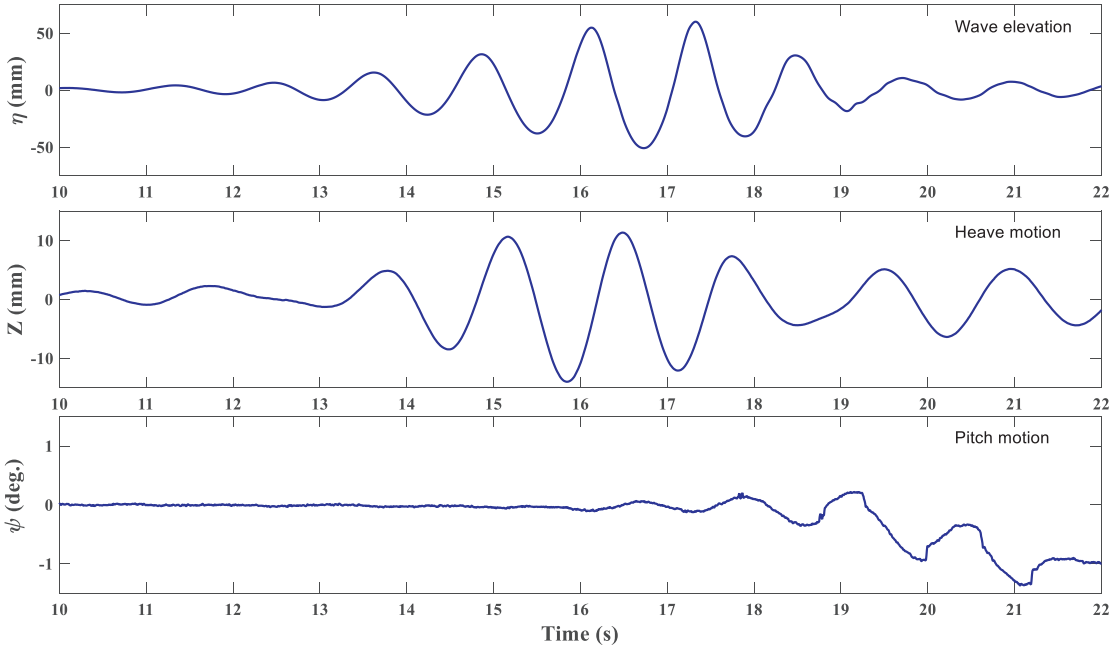

Fig. 10. Time history of wave and model's motions for condition 1 (Target η_{max} = 63.2 mm).

and wave length, this might have caused such a difference in the wave packet along the tank.

A sharp disturbance in pitch motion was observed in the test conditions 3–5 directly after the impact of the focused wave (time: 18–20 s in Figs. 11 and 12). Such a rapid spiked motion was most likely due to the loss of the air gap (negative air gap) between the wave and the deck underside, thereby the model experienced under deck slamming loads. Despite the large deck clearance of the model (120 mm) in comparison to η_{max}, there was an evidence from Fig. 13 (condition 5) that the model dynamic air gap was negative ($a = a_0 - \eta_{max} \pm Z \leq 0.0$ in which $a_0 = 120$ mm). In conditions 3–5, two wave-in-deck impact events occurred on the second and third crests of the focused wave packet. Impact one hit the mid-deck underside of the model and the second hit the underside area around the aft columns causing a significant amount of run-up on the rear columns (see Fig. 13). These consecutive wave impacts caused a significant negative stepped pitch motion; the wave impacted the model causing it to pitch about its centre of mass, and hence the air gap became negative.

It should be stressed that the tested conditions provided a consistent deck impact event in a very short period of time. This key strength of the focused wave technique; it is possible to create a specific sea state within a very short period. The time series recorded were only 20 s in length, which overcomes problems caused by wave reflections in the physical wave tanks. Using standard wave spectra for the testing of a model with the current model testing facilities does not ensure a set time and location of a design wave, potentially leading to refraction interfering or ineffective model placement. With a careful selection of wave celerity, it would be possible to obtain a much focused wave as shown by the progression of conditions one to five. As such using the presented focused wave could be considered efficient for predicting slamming loads on both floating and fixed structures.

The heave magnitude measured for each condition showed an expected trend in that the maximum values increased proportional to the focus wave amplitude. As shown in Fig. 14, the increasing wave amplitude had a proportionally increasing impact on the heave motion of the model in the positive and negative directions. Similarly, the pitching motion of the model increased in magnitude with the progressively larger wave sets. The general reaction of the model from one condition to the next was noted to increase in this manner (see Fig. 15). The cause would likely be the condensed yet increase energy for the wave packets between each wave set.

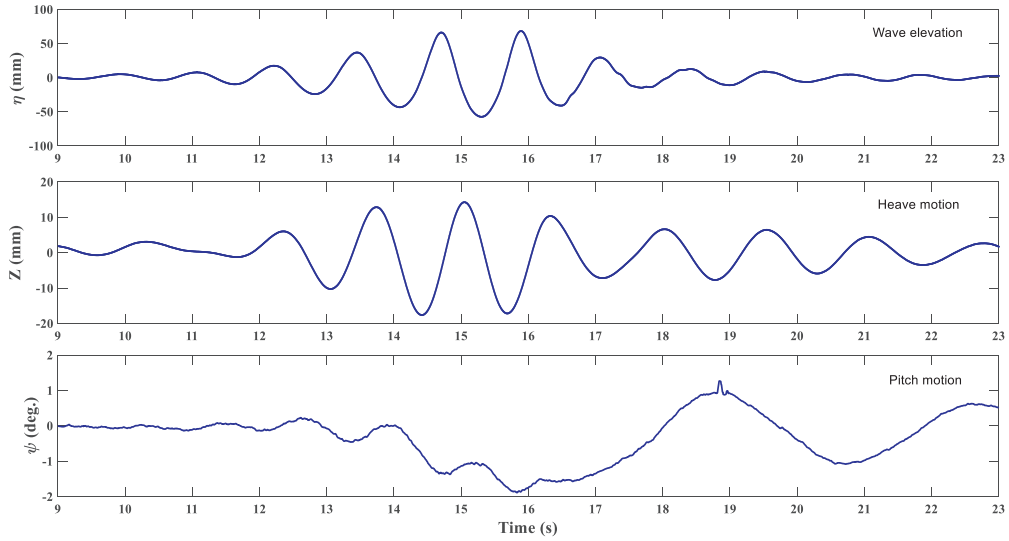

Fig. 11. Time history of wave and model's motions for condition 3 (Target η_{max} = 75.84 mm).

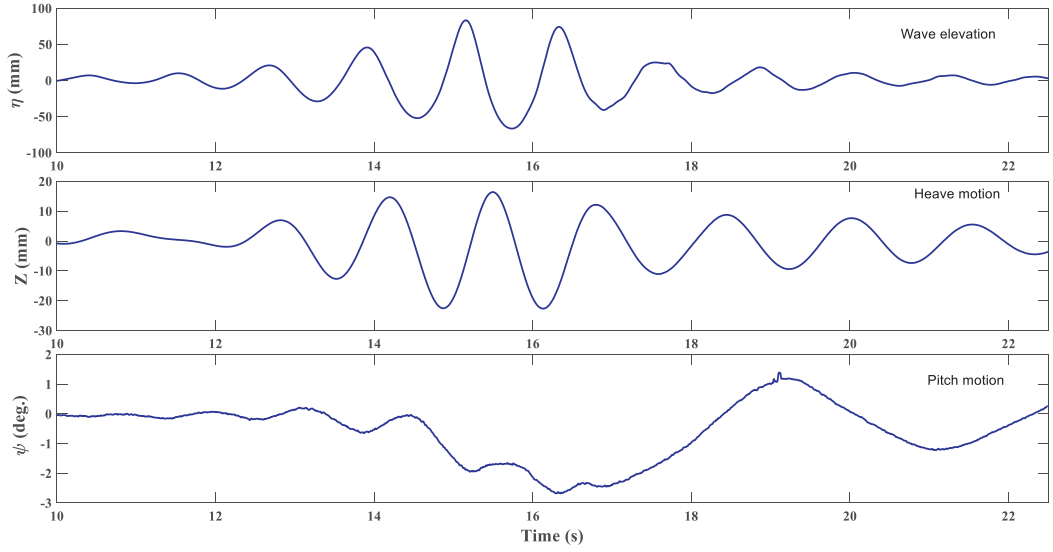

Fig. 12. Time history of wave and model's motions for condition 5 (Target η_{max} = 88.48 mm).

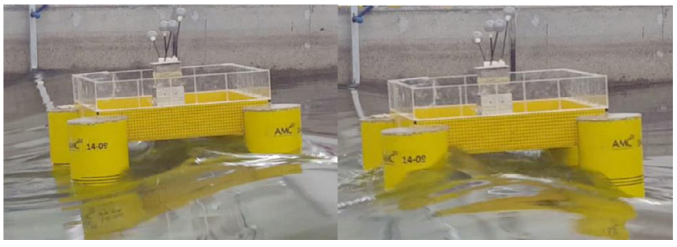

Fig. 13. Photographs of the model encountering large pitch motion and deck impact: mid-deck (left) and around the aft columns (right).

Among sets there is a notable increase in the steepness of the waves, this when coupled with larger amplitude and shorter time would cause the motion of the model. The design wave elevation error for all conditions was well within acceptable limits, not exceeding 4% as presented in Table 7. Overall, a linear correlation between η_{max} and model's motions was evident from the tested conditions. Increasing the number of test conditions and modelling more realistic extreme wave conditions such as the New Year wave are recommended for future work.

6. Conclusions

Using the NewWave theory, i.e., focused wave technique, a focused wave was created and applied to a generic model of semisubmersibles in the physical wave tank. The focused wave conditions used for testing were a scaled wave first used by Ning et al. [16] with an amplitude of 63.2 mm of the largest crest. The initial task was to apply the NewWave theory to wavemaker system through the use of user defined wavemaker displacement signals. Care was taken to assess the usability and reliability of this method, taking close

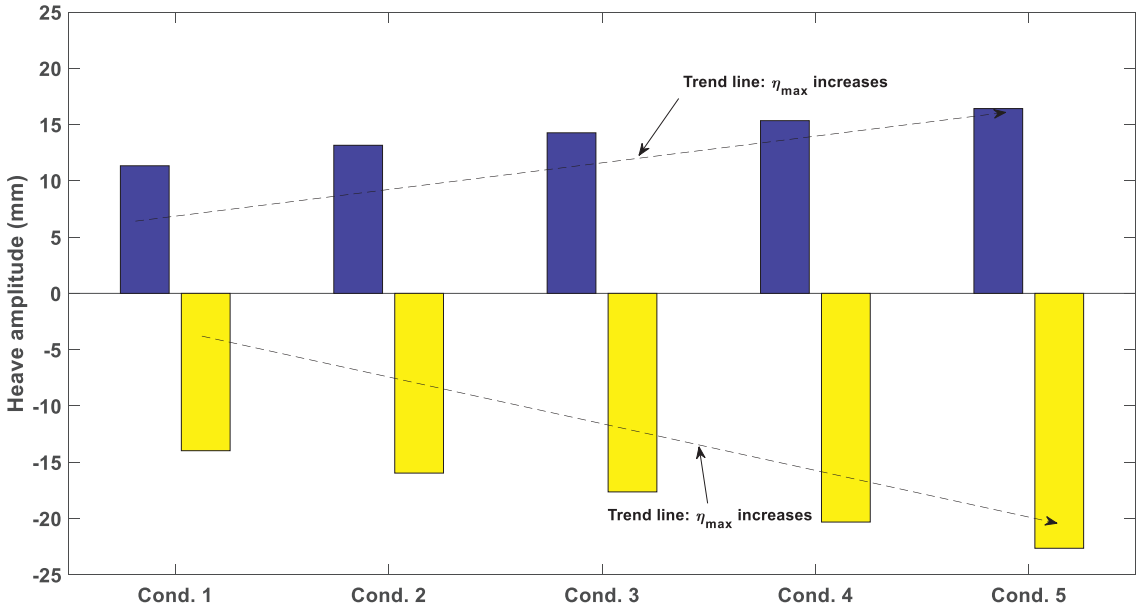

Fig. 14. Heave motion amplitude for all conditions.

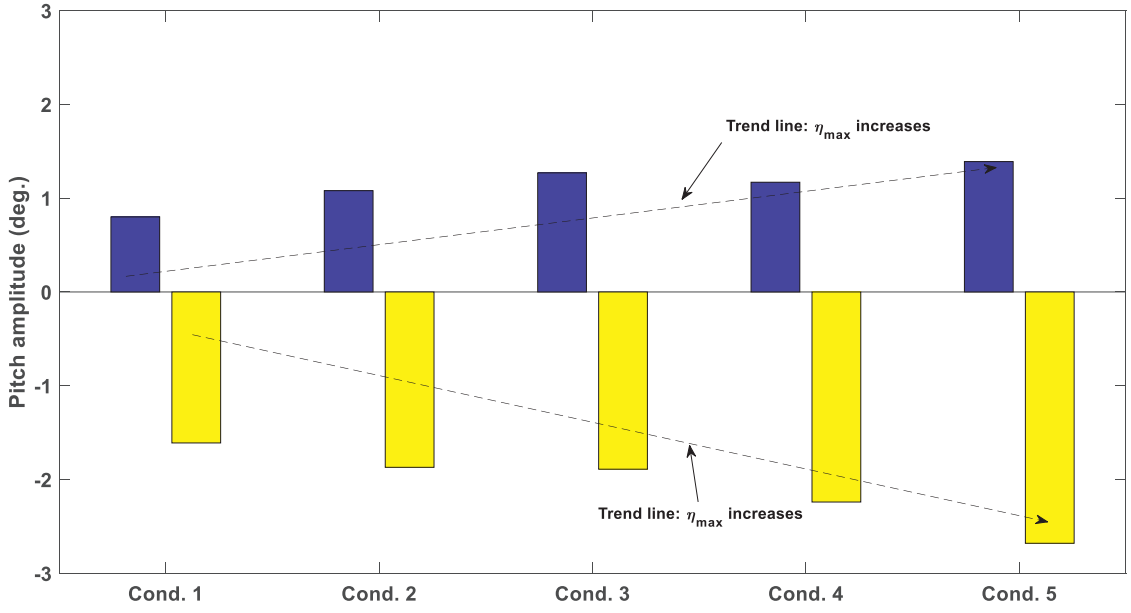

Fig. 15. Pitch motion amplitude for all conditions.

observation of the relatively low degree of error. The design focused wave was measured over 13 runs at four set points to assess wave slope, height and general qualitative pattern at different distances from the wavemaker paddle. The produced waves were consistent in pattern, showing a low degree of peak and slope error between runs. The calibration process highlighted the impact of nonlinear wave to wave interactions on the amplitude of the waves further away from the wavemaker paddle.

Testing the scaled model was undertaken using five progressively larger wave conditions. The base focused wave was taken from the calibration and increased by 10% for each progressive condition. Tracking the pitch and heave of the model analysis was taken of the model motions focusing on the repeatability and variation. It was found that the increasing energy of the increased amplitude waves caused a proportional increase in motions of the model. This culminated with the model experiencing a significantly large heave and pitch motion due to the higher condensed energy of the largest focused wave. The wave packet proved to be a reliable method for testing the dynamic response of offshore platforms at model scale with a high level of wave amplitude control, and hence it could be used to investigate the dynamic air gap of a floating structure.

Acknowledgements

The authors are grateful to Dr Shinsuke Matsubara for programming advice and to Professor Ning for his advice on using the NewWave theory.

References

[1] S. Haver, A Possible Freak Wave Event Measured at the Draupner Jacket January 1 1995 Rogue Waves 2004, 2004, pp. 1–8.
[2] T.A.A. Adcock, P.H. Taylor, S. Yan, Q. Ma, P.A.E.M. Janssen, in: Proceedings of the Royal Society A: Mathematical, Physical and Engineering Sciences, 2011.
[3] DNV GL, Strategic Research and Innovation Potion Paper 05-2015: Rogue Waves Impact on Ships and Offshore Structures, 2015.
[4] L. Bertotti, L. Cavaleri, Ocean Eng. 35 (1) (2008) 1–5.
[5] E.J. Ransley, School of Marine Science and Engineering, University of Plymouth, 2015, p. 253.
[6] C. Cui, et al., Ocean Eng. 54 (2012) 132–141.
[7] J. Touboul, et al., Eur. J. Mech.—B/Fluids 25 (5) (2006) 662–676.
[8] T. Baldock, C. Swan, P. Taylor, Philos. Trans. R. Soc. Lond. A: Math. Phys. Eng. Sci. 354 (1707) (1996) 649–676.
[9] J.R. Chaplin, Int. J. Offshore Polar Eng. 6 (02) (1996) 131–137.
[10] C. Schmittner, S. Kosleck, J. Hennig, in: ASME 2009 28th International Conference on Ocean, Offshore and Arctic Engineering, American Society of Mechanical Engineers, 2009.
[11] H. Fernández, et al., Coastal Eng. 93 (2014) 15–31.
[12] J. Cook, Localised Loadings on a Tension Leg Platform as a Result of Extreme Wave Events, Australian Maritime College, Launceston, 2011.
[13] P.S. Tromans, A.R. Anaturk, P. Hagemeijer, in: The First International Offshore and Polar Engineering Conference, International Society of Offshore and Polar Engineers, 1991.
[14] M.J. Cassidy, Non-linear Analysis of Jack-up Structures Subjected to Random Waves, University of Oxford, United Kingdom, 1999.
[15] N. Gao, J. Yang, W. Zhao, X. Li, Ships Offshore Struct. 11 (8) (2016).
[16] D. Ning, et al., Ocean Eng. 36 (15) (2009) 1226–1243.
[17] Y. Deng, et al., Coastal Eng. 114 (2016) 9–18.
[18] N. Gao, J. Yang, X. Tian, X. Li, Ships Offshore Struct. 12 (4) (2017).
[19] X. Lu, et al., in: ASME 2014 33rd International Conference on Ocean, Offshore and Arctic Engineering, American Society of Mechanical Engineers, 2014.
[20] J. Westphalen, et al., Ocean Eng. 45 (2012) 9–21.
[21] J. Westphalen, Extreme Wave Loading on Offshore Wave Energy Devices using CFD, University of Plymouth, 2011, p. 241.
[22] M. Cassidy, R.E. Taylor, G. Houlsby, Appl. Ocean Res. 23 (4) (2001) 221–234.
[23] Z.Z. Hu, et al., Natural Hazards Earth Syst. Sci. 11 (2) (2011) 519–527.
[24] Y. Deng, et al., Ocean Eng. 118 (2016) 83–92.
[25] P.J. Beresford, HR WaveMaker Wave Generation Control Program: Software Manual, HR Wallingford, Oxon, 2003.
[26] F. Ursell, R.G. Dean, Y. Yu, J. Fluid Mech. 7 (01) (1960) 33–52.